The aromaticity of the [Re 3(μ-X) 3X 9] 3- clusters, X = Cl, Br, i

ARTICLE *in* CHEMICAL PHYSICS LETTERS · JULY 2012

Impact Factor: 1.9 · DOI: 10.1016/j.cplett.2012.07.033

Chemical Physics Letters 545 (2012) 50–53

Contents lists available at SciVerse ScienceDirect

Chemical Physics Letters

journal homepage: www.elsevier.com/locate/cplett

The aromaticity of the $[Re_3(\mu\text{-}X)_3X_9]^{3-}$ clusters, X = Cl, Br, I

Leonor Alvarado-Soto [a], Eduardo Schott V [b], Ximena Zarate [b], Ramiro Arratia-Pérez [b], Rodrigo Ramirez-Tagle [a,*]

[a] Universidad Bernardo ÓHiggins, General Gana 1780, 8370854 Santiago, Chile
[b] ReMoPh Group, Universidad Andrés Bello, Av. República 275, 8370146 Santiago, Chile

ARTICLE INFO

Article history:
Received 12 June 2012
In final form 15 July 2012
Available online 25 July 2012

ABSTRACT

The results of this Letter reveals that the $[Re_3(\mu\text{-}Cl)_3Cl_9]^{3-}$, $[Re_3(\mu\text{-}Br)_3Br_9]^{3-}$, $[Re_3(\mu\text{-}I)_3I_9]^{3-}$ clusters exhibit aromaticity and that spin–orbit effect decreases the aromaticity due to the fact that the $5d_{3/2}$ spinors are more contracted than the scalar 5d orbitals. The $[Re_3(\mu\text{-}I)_3I_9]^{3-}$ and $[Re_3(\mu\text{-}Br)_3Br_9]^{3-}$ clusters are the most aromatic clusters. This can be explained by the $np_{1/2}$ and $np_{3/2}$ spinors radial expectation ($\langle r \rangle$) values which follows the Cl < Br < I sequence. Thus, the most extended spinors correspond to I and Br ligands, as indicated in the ELF plots. Furthermore we carried out TDDFT calculations which agrees with the fact that $[Re_3(\mu\text{-}I)_3I_9]^{3-}$ should show the highest value of aromaticity.

1. Introduction

Frequently the phenomenon of electronic delocalization is used for understanding the unusual stability of planar cyclic molecules that exhibit delocalized π-bonds. Initially, aromaticity was developed only for organic compounds, but today this concept has been extended to a large number of compounds, such as, inorganic and organometallic complexes [1–4]. In recent years we have seen the resurgence in the development of various evaluation criteria of aromaticity of a molecular system, Schleyer and co-workers developed the concept of Nucleus-Independent Chemical Shift (NICS), which was tested in the Al_4^{2-} dianion [5,6]. Also, the study of aromaticity in metallic clusters was conducted by a combination of photoelectron spectroscopy and *ab initio* calculations which showed evidence of *d*-orbital aromaticity in 4*d* and 5*d* transition metallic oxide clusters, namely $[M_3O_9]^{2-}$ (M = Mo, W) [7–9]. Although, the term d-orbital aromaticity was first coined by Tsipis and co-workers [10].

Moreover, the NICS index has become a popular probe of delocalization in a variety of molecules and is now accepted as an efficient method to evaluate aromaticity, however, some results must be taken with caution [11,12]. Negative NICS values in interior positions of rings or cages indicate the presence of induced diatropic ring currents which is interpreted as aromaticity, whereas positive values at each point denote paratropic ring currents and is interpreted as antiaromaticity [12,13]. Many attempts to evaluate the electron delocalization in inorganic systems by magnetic criteria have been made [1–6,12], where, a variety of theoretical calculations including scalar relativistic effects with pseudopotentials have been reported to estimate NICS values [1–6,13,14]. The first good evidence of metalloaromaticity was recognized more than a decade ago by Robinson in the Ga_3^{2-} ring due to the delocalization of two π electrons and thus it becomes isoelectronic with the aromatic triphenylcyclopropenium species [3]. A year later, the aromatic character of the gallium ring was supported by NICS calculations, where the NICS(0) value was evaluated at the center of the plane and the NICS(1) value was evaluated 1 Å out the plane, (NICS(0) = −45.4 ppm and NICS(1) = −23.5 ppm) at the GIAO-B3LYP/6-311+G*//B3LYP/6-311+G* level [4].

Recently, the study of aromaticity has included most of the relativistic effects, except quantum electrodynamics corrections. For example, the role of spin–orbit (SO) coupling in Re_3X_9 clusters was estimated by two-component ZORA Hamiltonian, which is an approximation to the Dirac equation and includes scalar relativistic and SO corrections [15,16]. A four-component formalism using the Dirac Hamiltonian has been recently used to study aromaticity via the induced current density in C_5H_5E (E = N, P, As, Sb, Bi) and $[(HtAc)_3(\mu2\text{-}H)_6]$, $[(HtTh)_3(\mu2\text{-}H)_6]^+$ and $[(HtPa)_3(\mu2\text{-}H)_6]$ clusters, showing good agreement with previously reported data for the NICS values [11,17].

Here we report the calculated electronic structure, NICS values, electronic transitions and the evaluation of the electron localization function (ELF) to characterize the aromaticity in the $[Re_3(\mu\text{-}X)_3X_9]^{3-}$ clusters with X = Cl, Br, I (see Figure 1) by taking into account scalar and SO relativistic effects.

2. Computational details

Our calculations for the $[Re_3(\mu\text{-}X)_3X_9]^{3-}$ (X = Cl, Br, I) clusters were carried out using the Amsterdam density functional (ADF) code [18]. The SO and scalar relativistic effects were incorporated

* Corresponding author.
E-mail addresses: rodrigoramireztagle@gmail.com, rramirez@ubo.cl (R. Ramirez-Tagle).

0009-2614/$ - see front matter © 2012 Elsevier B.V. All rights reserved.
http://dx.doi.org/10.1016/j.cplett.2012.07.033

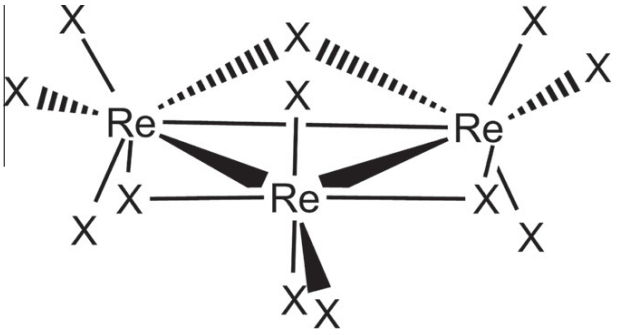

Figure 1. Scheme of the $[Re_3(\mu\text{-}X)_3X_9]^{3-}$ clusters where X = Cl, Br, I.

via the zeroth order regular approximation (ZORA Hamiltonian) [19–21]. All the molecular structures were fully optimized via the analytical energy gradient method implemented by Verluis and Ziegler employing the local density approximation (LDA) within the Vosko–Wilk–Nusair parametrization for local exchange correlations [21,22]. The molecular structure is characterized by having a triangle of Re atoms plus three bridges (μ) halides atoms in the same plane and six apical halides atoms (out of the plane) [23–26]. The diagonal $NICS_{zz}$ values were calculated using the generalized gradient approximation (GGA) with the OPBE functional [14], which is specially designed for the calculations of chemical shifts and other magnetic properties. The excitation energies were estimated using the time dependent perturbation density functional theory (TDDFT), using the model of Van Leeuwen and Baerends (LB94) which targeted the long-range behavior of the XC potential and indeed improved properties that critically depend on the long-range behavior [27]. Solvation effects were modeled by the conductor-like screening model for real solvents (COSMO) using acetonitrile as solvent for all the calculations [28,29]. All the calculations were carried out using standard Slater-type-orbital (STO) basis sets with triple-ς quality plus double polarization functions (TZ2P) for the all the atoms [30].

3. Results and discussion

The geometry optimizations, which include scalar and SO corrections, were performed in vacuum. According to our calculations, the $[Re_3(\mu\text{-}X)_3X_9]^{3-}$ clusters have D_{3h} symmetry and exhibits a diamagnetic ground state. The nuclear magnetic resonance (NMR) parameters were calculated for a ghost atom placed at the center of the ring, where the NICS value is the negative value of the isotropic magnetic shielding constant. The NICS(0) values at the center of the ring formed by the metals is mostly influenced by σ-bonds, whereas the NICS(1) values calculated 1 Å above or below the plane are mostly affected by the π-bonds. Although spin–orbit coupling mixes the σ and π states, as shown before by us [15,16].

A plot for the values of the scan performed for the $NICS_{zz}$ values of the metallic ring up to 4 Å over and below the ring plane is depicted in Figure 2, where we observe a clear picture of the ring currents in the title aromatic systems. The current calculations show large negative $NICS_{zz}$ values for each $[Re_3(\mu\text{-}X)_3X_9]^{3-}$ cluster which arises due to their high 5d(Re) and 5p(X) delocalization. It can be extracted from Figure 2, that the $NICS_{zz}(1)$ values are higher than $NICS_{zz}(0)$ with scalar ZORA calculations with and without SO (ZORA + SO) corrections, which indicates that the greatest contribution to the delocalization is mostly of π character. However, as can be seen from Figure 2, in all the clusters the SO effects decrease their aromaticity. This is due to the fact that the $5d_{3/2}$ spinors (which are 66% occupied) are more contracted than the $5d_{5/2}$ spinors [16]. In

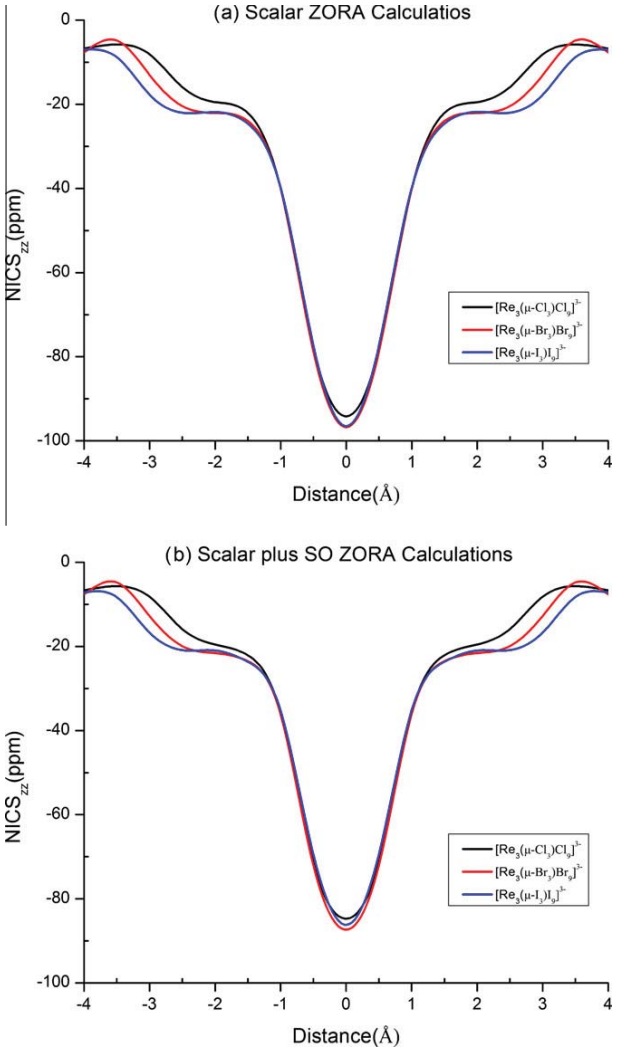

Figure 2. $NICS_{zz}$ scan profile (NICS in ppm, R in Å) for the all the clusters.

Table 1
The atomic spinors $\langle r\rangle(np_j)$ values (a.u.)[30].

X	Cl	Br	I
$\langle r\rangle(np_{1/2})$	1.835	2.074	2.402
$\langle r\rangle(np_{3/2})$	1.844	2.118	2.516

Table 2
NICS values at (0.0) Å (0) and (1.0) Å (1) below the plane of the ring.

Complex	Th.[a]	NICS (0)	NICS (1)
$[Re(\mu\text{-}Cl_3)Cl_9]^{3-}$	Scal.	−40.0	−94.2
	SO	−35.8	−84.7
$[Re(\mu\text{-}Br_3)Br_9]^{3-}$	Scal.	−40.0	−96.7
	SO	−36.0	−87.4
$[Re(\mu\text{-}I_3)I_9]^{3-}$	Scal.	−39.8	−96.5
	SO	−35.2	−86.2

[a] Theory level (Th.): Scalar ZORA (Scal.) and SO + ZORA (SO).

relativistic theory is known that 5d orbitals split by spin–orbit coupling into the $5d_{3/2}$ and $5d_{5/2}$ spinors, being the $5d_{3/2}$ spinors more contracted that the scalar 5d orbitals [31]. Thus, the delocalization

Table 3
Calculated transition energies (eV), oscillator strength (f) and active molecular orbitals and their contributions (%) from TDDFT + SO for the two lowest energy transitions.

Complex	eV	f	Transition, orbital contribution (%)			
$[Re(\mu\text{-}Cl_3)Cl_9]^{3-}$	0.8598	1.12E-06	22 e1/2	↔	23 e5/2	59
			22 e3/2	↔	23 e5/2	38
	0.9022	8.04E-05	22 e1/2	↔	23 e5/2	98
			22 e3/2	↔	23 e3/2	1
$[Re(\mu\text{-}Br_3)Br_9]^{3-}$	0.8469	1.07E-05	22 e1/2	↔	23 e5/2	83
			21 e1/2	↔	23 e5/2	15
	0.9011	1.32E-04	22 e1/2	↔	23 e5/2	46
			22 e3/2	↔	23 e5/2	36
$[Re(\mu\text{-}I_3)I_9]^{3-}$	0.3923	9.96E-04	22 e3/2	↔	23 e5/2	96
			22 e1/2	↔	23 e5/2	4
	0.4764	5.59E-05	22 e1/2	↔	23 e5/2	98
			20 e1/2	↔	23 e5/2	1

and $NICS_{zz}$ values decreases and therefore the aromaticity decreases due to SO effects.

It can be also observed from Figure 2 and from Table 2, that the $[Re_3(\mu\text{-}I)_3I_9]^{3-}$ and $[Re_3(\mu\text{-}Br)_3Br_9]^{3-}$ clusters are the most aromatic. This can be explained invoking the spinors radial expectation $\langle r \rangle$ values of the halides Br and I. The radial extension of $np_{1/2}$ and $np_{3/2}$ spinors follows the sequence Cl < Br < I, as shown in Table 1. Thus, the most extended spinors correspond to 'I' ligands and hence, the $[Re_3(\mu\text{-}I)_3I_9]^{3-}$ and $[Re_3(\mu\text{-}Br)_3Br_9]^{3-}$ clusters should have the largest electronic delocalization and consequently the largest aromaticity. The incorporation of axial halide ligands in the $[Re_3X_9]$ systems [32] seems to have the effect of keeping the σ aromaticity constant and a decrease of the π aromaticity.

To corroborate our results we carried out TDDFT calculations including SO corrections to characterize the lowest energy transitions of the complexes. It has been shown that the chemical shielding tensors are connected via a common description in terms of paramagnetic and diamagnetic contributions [33–35]. Corminboeuf et. al. have employed symmetry-based criteria to validate orbital contributions to GIAO NICS values [33]. The idea is that the NICS values are determined by the accessibility of excited electronic states, and the paramagnetic/diamagnetic nature of the excitation is determined by symmetry selection rules and also by the magnitude of the transition energies. For symmetric molecules, diatropic orbital contributions to the NICS are determined by the existence of (electric) dipole-allowed occupied-to-unoccupied orbital transitions (translational x or y symmetry), whereas paratropic contributions are given by (magnetic) rotationally allowed transitions which have the R_z symmetry when a magnetic field perpendicular to the molecular XY plane is applied. In summary, the character of diamagnetic or paramagnetic is given by the competition between translational and rotational allowed excitations. The excitation energies, that could contribute to the diatropic part of the NICS, can be estimated based on TD-DFT calculations which by group theory definition are dipole-allowed (translational (x, y) allowed) transitions. Our TDDFT calculations include the SO interaction, for which double point group D^*_{3h} must be considered [36]. In Table 3 we have listed the two lowest energy excitations involving the frontier molecular orbitals. The excitations with a zero oscillator strength value are forbidden by electric dipole double group symmetry. All the values listed in Table 3 were calculated with the model LB94 functional which is specially designed for TDDFT calculations, because it possesses a correct $1/r$ asymptotic behavior [27]. The oscillator strengths and excitation energies of the dipole allowed transitions in Table 3 decrease systematically in the order Cl > Br > I. This means that the diatropic contribution to the NICS decreases in that order. These facts could also explain the difference in aromaticity showed by the different clusters.

To complement the study of these clusters, we carried out the calculation of the ELF. The ELF plots in the plane containing the metallic central core of the cluster are shown in Figure 3. The electronic delocalization in each cluster is clearly illustrated where the same trend described above is observed.

4. Conclusions

Our calculations have shown that the $[Re_3(\mu\text{-}Cl)_3Cl_9]^{3-}$, $[Re_3(\mu\text{-}Br)_3Br_9]^{3-}$, $[Re_3(\mu\text{-}I)_3I_9]^{3-}$ clusters exhibit high aromaticity and that the SO effect decreases the aromaticity due to the fact that the $5d_{3/2}$ spinors are more contracted than the scalar 5d orbitals. The $[Re_3(\mu\text{-}I)_3I_9]^{3-}$ is the most aromatic clusters which may be explained by the $np_{1/2}$ and $np_{3/2}$ halide radial expectation ($\langle r \rangle$) values which follows the sequence Cl < Br < I. Thus, the most extended spinors correspond to iodide ligands and hence the $[Re_3(\mu\text{-}I)_3I_9]^{3-}$ and $[Re_3(\mu\text{-}Br)_3Br_9]^{3-}$ clusters should have the largest electronic delocalization and consequently the largest aromaticity, as noticed in the ELF plots. Furthermore, the TDDFT calculations for all the clusters including the SO corrections, indicate a red shift of the lowest transitions, which might also explain the difference in aromaticity showed by each cluster, where it is expected that $[Re_3(\mu\text{-}Cl)_3Cl_9]^{3-}$ is less aromatic and that $[Re_3(\mu\text{-}I)_3I_9]^{3-}$ should be the most aromatic.

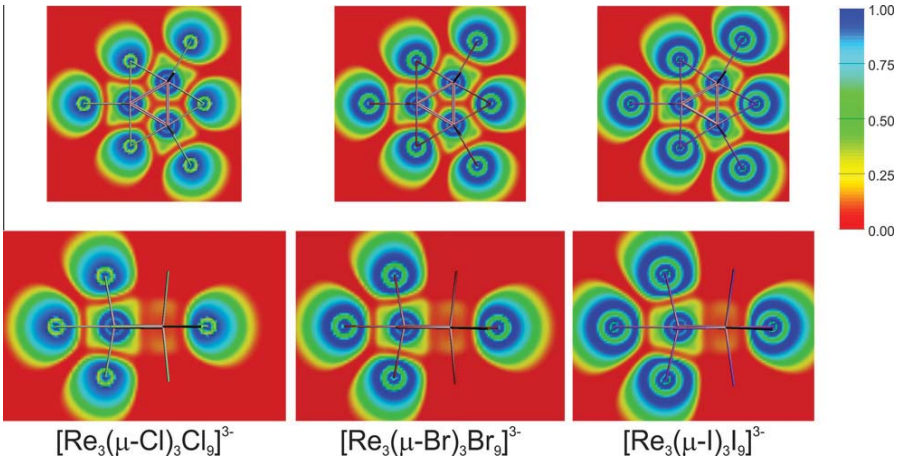

Figure 3. ELF plots of the three clusters.

Acknowledgements

This Letter has been supported by Projects AT24100024, FONDECYT 3100048 and 1110758, UNAB-DI-17-11/R, and NUCLEUS MILLENNIUM No. P07-006-F.

References

[1] A.E. Kuznetsov, A.I. Boldyrev, X. Li, L.-S. Wang, J. Am. Chem. Soc. 123 (2001) 8825.
[2] A.D. Phillips, P.P. Power, J. Cluster Sci. 13 (2002) 569.
[3] X.-W. Li, W.T. Pennington, G.H. Robinson, J. Am. Chem. Soc. 117 (1995) 7578.
[4] Y. Xie, P.R. Schreiner, H.F. Schaefer, X.-W. Li, G.H. Robinson, J. Am. Chem. Soc. 118 (1996) 10635.
[5] P. von Ragué Schleyer, C. Maerker, A. Dransfeld, H. Jiao, N.J.R. van E. Hommes, J. Am. Chem. Soc 118 (1996) 6317–6318.
[6] Z. Chen, C. Corminboeuf, T. Heine, J. Bohmann, P.V.R. Schleyer, J. Am. Chem. Soc. 125 (2003) 13930.
[7] X. Li, A.E. Kuznetsov, H.-F. Zhang, A.I. Boldyrev, L.-S. Wang, Science (New York, NY) 291 (2001) 859–861.
[8] A.E. Kuznetsov, K.A. Birch, A.I. Boldyrev, X. Li, H.-J. Zhai, L.-S. Wang, Science (New York, NY) 300 (2003) 622–625.
[9] X. Huang, H.-J. Zhai, B. Kiran, L.-S. Wang, Angew. Chem. Int. Ed. 44 (2005) 7251.
[10] A.C. Tsipis, C.A. Tsipis, J. Am. Chem. Soc. 125 (2003) 1136.
[11] R. Ramírez-Tagle, L. Alvarado-Soto, R. Arratia-Perez, R. Bast, L. Alvarez-Thon, J. Chem. Phys. 135 (2011) 104506.
[12] A.I. Boldyrev, L.-S. Wang, Chem. Rev. 105 (2005) 3716.
[13] Z. Chen, C.S. Wannere, C. Corminboeuf, R. Puchta, P.V.R. Schleyer, Chem. Rev. 105 (2005) 3842.
[14] Y. Zhang, A. Wu, X. Xu, Y. Yan, Chem. Phys. Lett. 421 (2006) 383.
[15] L. Alvarado-Soto, R. Ramírez-Tagle, R. Arratia-Perez, J. Phys. Chem. A 113 (2009) 1671.
[16] L. Alvarado-Soto, R. Ramírez-Tagle, R. Arratia-Perez, Chem. Phys. Lett. 467 (2008) 94.
[17] R. Bast, J. Jusélius, T. Saue, Chem. Phys. 356 (2009) 187.
[18] T.N. Vrije Universiteit, Amsterdam, (2009).
[19] E. van Lenthe, E.J. Baerends, J.G. Snijders, J. Chem. Phys. 101 (1994) 9783.
[20] G.T. Velde, F.M. Bickelhaupt, E.J. Baerends, C.F. Guerra, J. Comput. Chem. 22 (2001) 931.
[21] L. Versluis, T. Ziegler, J. Chem. Phys. 88 (1988) 322.
[22] S.H. Vosko, L. Wilk, M. Nusair, Can. J. Phys. 58 (1980) 1200.
[23] J. Bennett, F.A. Cotton, B.M. Foxman, Inorg. Chem. 7 (1968) 1563.
[24] M.B. Hursthouse, K.M.A. Malik, J. Chem. Soc., Dalton Trans. (1978) 1334–1337.
[25] M.A. Bush, P.M. Druce, M.F. Lappert, J. Chem. Soc., Dalton Trans. (1972) 500–503.
[26] J.A. Bertrand, F.A. Cotton, W.A. Dollase, Inorg. Chem. 2 (1963) 1166.
[27] R. van Leeuwen, E.J. Baerends, Phys. Rev. A 49 (1994) 2421.
[28] A. Klamt, V. Jonas, J. Chem. Phys. 105 (1996) 9972.
[29] A. Klamt, J. Phys. Chem. 99 (1995) 2224.
[30] J.G. Snijders, P. Vernooijs, E.J. Baerends, Atom. Data Nucl. Data Tabl. 26 (1981) 483.
[31] C.C. Lu, T.A. Carlson, F.B. Malik, T.C. Tucker, C.W. Nestor, Atom. Data Nucl. Data Tabl. 3 (1971) 1.
[32] A.C. Tsipis, I.G. Depastas, E.E. Karagiannis, C.A. Tsipis, J. Comput. Chem. 31 (2010) 431.
[33] C. Corminboeuf, R.B. King, P.V.R. Schleyer, ChemPhysChem 8 (2007) 391.
[34] W. Bieger, G. Seifert, H. Eschrig, G. Grossmann, Chem. Phys. Lett. 115 (1985) 275.
[35] P. Lazzeretti, Prog. Nuc. Magn. Reson. Spec. 36 (2000) 1.
[36] G.F. Koster, J.O. Dimmock, R.G. Wheeler, H. Statz, The Properties of the Thirty-Two Point Groups, MIT, Cambridge, MA, 1963, p. 104.